

An Efficient Neural-Network based Approach to Automatic Ship Docking

Yonghui Shuai^a, Guoyuan Li^{b,*}, Xu Cheng^b, Robert Skulstad^b, Jinshan Xu^a,
Honghai Liu^a, Houxiang Zhang^b

^a*Zhejiang University of Technology, Zhejiang, 310014 PR China*

^b*Norwegian University of Science and Technology, Aalesund, 6009 Norway*

Abstract

Automatic ship docking is one of the applications of autonomous ships. How to realize autonomous low-speed maneuver under environmental disturbances for docking is the fundamental problem at present. This paper presents an efficient approach based on artificial neural network (ANN) for automatic ship docking. The problem is formulated and well-modelled for simulating ship docking operation. A joystick implementation in simulation provides manual maneuvering and thus enables collection of sufficient and reliable data from successful maneuvers. To keep consistent with the manual control, an ANN with two parallel structure is proposed to control the ship's thrust and rudder, respectively. Feature selection technique and genetic algorithm (GA) are utilized to optimize the structure and reduce the training cost. Numerical simulations under different environmental disturbances, including no wind, constant wind and dynamic wind are carried out. The results show the ship is able to reach the dock smoothly, which confirms the effectiveness of the proposed approach.

Keywords: autonomous ship, ship docking, feature selection, neural network, genetic algorithm

*Corresponding author

1. Introduction

Digitization is a major agenda in the development strategy of the European shipbuilding industry, which promotes technological innovation and economic growth. This agenda points out that the first task is to achieve ship autopilot characterized by strong adaptability to sea conditions, low energy consumption, and high safety performance. Automatic ship docking is considered an essential application of ship autopilot. Ship docking is a challenging manoeuvring task for captains. During the docking process, the captain needs to know the ship's current state and estimates its future state based on the manoeuvrability of the ship. The ship is suggested to be sailed at low speed to avoid collision with the dock and other vessels; but low speed will sharply reduce the ship's manoeuvrability and increase control complexity.

To address the above challenges, attempts have been made to design advanced controllers using knowledge of nonlinear control theory [1, 2, 3] and fuzzy theory [4, 5]. However, it is hard to construct nonlinear mathematical models and define fuzzy rules for ship docking since any unpredictable situations including weather influences and other vessels' disturbances may arise. In such a case, an ANN-based approach with the ability to learn the underlying nature from manoeuvring data, provides a potential solution for automatic ship docking. In principle, the robustness of this approach depends not only on the ANN's structure but also on the training data. The training data can be either from real ship docking operation, or from reliable simulation. The former has high reliability, but is difficult to be collected under different environmental disturbances; the latter is most frequently used because of its high efficiency, and as long as the fidelity of modeling ship docking operation is good enough, the reliability of the training data is guaranteed.

In this paper, we propose a new ANN-based approach to achieve automatic ship docking under different environmental disturbances. The main contributions of this paper can be summarized as follows:

- 1) A ship docking simulation module with complete ship-environment models

31 is established for generating reliable docking data.

32 2) The feature selection technique is applied to provide optimal inputs for
33 the ANN.

34 3) The ANN-based approach with two parallel structure optimized by genetic
35 algorithm is verified to be able to dock the ship under different environ-
36 mental disturbances.

37 The present paper is organized as follow. Section II is a brief overview of
38 related work. In Section III, a ship docking simulation module including ship
39 mathematical model and wind disturbance model is established. In section IV,
40 the proposed ANN-based approach, from data collection, feature selection, to
41 ANN construction and optimization, is introduced in detail. Section V presents
42 the docking results of the approach under different environmental disturbances.
43 Conclusions and future work are given in Section VI.

44 2. Related work

45 The first automatic ship berthing system based on ANN was demonstrated
46 in the 1990's by H. Yamato [6]. Later, Zhang et al. developed an automatic
47 ship-berthing system using a multivariate neural network based controller [7].
48 The pre-planned birthing path was determined as the input of the controller.
49 However, the authors did not introduce how to set the berthing path. In 2001,
50 Im and Hasegawa proposed a parallel neural network based controller to control
51 ship thrust RPM and rudder [8]. The experimental results demonstrated the
52 proposed parallel neural network-based controller could eliminate the effects of
53 slight wind and current, but failed to manipulate the ship to the destination in
54 harsh environment. To address this challenge, a motion recognition method was
55 utilized to cope with environmental impacts [9]. The method succeeded to com-
56 pensate the crosswind disturbance, but still failed when the wind comes from the
57 direction of the bow. Nguyen and Jung explored the adaptive neural networks to
58 achieve automatic ship berthing [10]. Recently, Zhang et al. proposed a robust

59 adaptive neural network approach based on the navigation dynamic deep-rooted
60 information to reconstruct the lumped uncertainties caused by unknown ship
61 dynamics and external disturbances [11].

62 The above researches focused more on the structure design of the ANN
63 controller; whilst none of them tried to generate training data with different
64 constraints by using an algorithm to improve the applicability of the ANN con-
65 troller. In fact, there have been attempts in training data generation. In 2007,
66 Ohtsu et al. proposed a new solution using nonlinear programming method
67 to generate minimum time ship manoeuvring data [12]. Hasegawa et al. first
68 attempted to use a nonlinear programming language (NPL) to generate ship
69 berthing data with restricted conditions [13]. Ahmed and Hasegawa followed
70 the research and first proposed the concept of virtual windows which is used to
71 ensure the consistency of training data [14, 15, 16, 17]. The NPL method allows
72 the user to define non-equal constraints by setting rudder angle as the optimal
73 variable and the time as an objective function. However, excessive restrictions
74 are defined as termination conditions in these researches when using the NPL
75 method, which causes fluctuation of rudder angle commands.

76 Nonlinear model prediction algorithm is another solution for optimal berthing
77 data generation, but requires higher computational resources to obtain the op-
78 timal maneuver path [18]. However, taking advantages of graphics processing
79 unit, the method can be executed in parallel, which makes real-time optimal
80 control feasible [19]. For example, Mizuno et al. proposed a quasi-real-time
81 optimal control system composed of a multiple shooting algorithm for docking
82 data generation and a nonlinear model predictive controller for path following
83 under wind disturbance [20].

84 There are also researches that directly use real ship docking data obtained
85 by experienced captains who successfully maneuver the ship into the berth, to
86 train neural network based controllers [21, 22]. But the method is not applica-
87 ble to general docking operation, as it is difficult to collect large number of real
88 ship docking data under different cases of environmental disturbances for train-
89 ing. To achieve the generality of ANN based docking in different environment

disturbances, we propose a new automatic ship docking strategy that employs a ship docking simulation platform to generate reliable docking data and an ANN-based approach with optimized parallel structure to manoeuvre ships into the dock.

3. Docking problem statement and simulation model

3.1. Docking problem statement

Slow speed, planning, on-board sensing equipment and control approach play key roles in ship docking. Kose et al. proposed two requirements to ensure ship safety according to the manoeuvring procedures followed by the captain in the actual docking of ships [23]. The first one is that the destination for docking should be at some distance away the dock instead of completely at the dock. The second one is that the captain has enough time to plan a good manoeuvre in any critical situation. To meet these two requirements, the whole process can be divided into two phases as shown in Fig. 1. The first is the ballistic phase. It utilizes the main thrusters and rudder for course changing, speed adjustment, and stopping. The second phase is to use tunnel thrusters to achieve side push.

In this paper, we focus on the first phase of the docking operation. It is assumed that the ship starts from a stationary state and maneuvers towards the port in low speed. The ship will dock in parallel to the port with zero velocities when it arrives at the destination. Moreover, three different sea conditions, including no wind, constant wind and dynamic wind, are considered for the docking problem.

In Fig. 1, $\{n\} = (x_N, y_N)$ is the North-East coordinate system, and its coordinate values can be obtained from the Global Positioning System (GPS). $\{d\} = (x_o, y_o)$ is called the north-up coordinate system which includes the heading angle and distance from ship to dock [22]. In this paper, all simulations are performed in the north-up coordinate system. The merit of using the north-up coordinate system is to control the ship into other different docks without re-

119 training the controller. $\{b\} = (x_b, y_b)$ represents the body coordinate system.

120 The notation for the marine vessel in Fig. 1 is shown in Table 1.

Table 1: The notation for marine vessels

Symbol	Description
G	The center of gravity
β_w, V_w	Relative wind direction and speed expressed in $\{d\}$
u, v, r	Surge, sway and yaw velocities expressed in $\{b\}$
x, y, ψ	Position and heading expressed in $\{d\}$
x_n, y_n, ψ_n	Position and heading expressed in $\{n\}$

121 3.2. Ship mathematical model

The study of ship dynamics consists of two parts: kinematics, which overcomes geometrical problems of motion; and kinetics, which analyzes the relationship between force and motion. Ship movement is expressed in six degrees

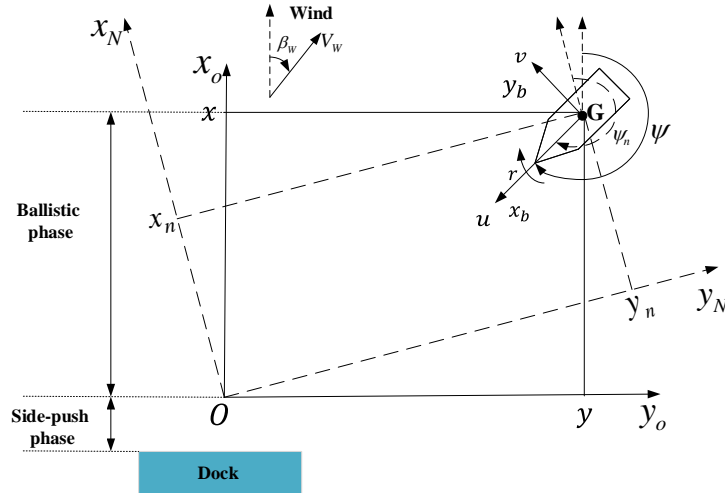


Figure 1: Coordinate systems for ship docking.

of freedom (DOF) which includes surge, sway, heave, roll, pitch and yaw [24]. For a surface ship, as shown in Fig. 1, it is only necessary to study the motion in three DOF, namely, the surge, sway and yaw. In this study, the maneuver model group (MMG) is used to describe ship motion, in which the hydrodynamic forces and moments acting on the ship are divided into modular components such as hull, rudder and propeller. The following is an MMG-based mathematical model considering wind influence [25]:

$$\begin{aligned}(m + m_x)\dot{u} + (m + m_y)vr &= X_H + X_P + X_R + X_W \\ (m + m_y)\dot{v} + (m + m_x)ur &= Y_H + Y_P + Y_R + Y_W \\ (I_{ZZ} + J_{ZZ})\dot{r} &= N_H + N_P + N_R + N_W\end{aligned}\quad (1)$$

where m is the ship mass; m_x, m_y are the added mass in surge, sway direction; I_{ZZ} is the mass moment of inertia; J_{ZZ} is the added mass moment of inertia; X, Y and N denote surge force, sway force and yaw moment; H, P, R and W are the symbols that represent hull, propeller, rudder and wind. The propeller and rudder are power-providing devices of ship, so X_P, Y_P, N_P, X_R, Y_R and N_R are the control inputs; and the ship velocities u, v, r are the control outputs for Eq. (1).

X_h, Y_h and N_h represent the hydrodynamic forces and moment acting on the ship hull, which are defined as [26]:

$$\begin{aligned}X_H &= \frac{\rho}{2} L d U^2 (X'_{\beta r} \sin \beta + X'_{uu} \cos^2 \beta \frac{rL}{U}) \\ Y_H &= \frac{\rho}{2} L d U^2 (Y'_\beta + Y'_r \frac{rL}{U} + Y'_{\beta\beta} \beta |\beta| + Y'_{rr} \frac{rL}{U} |\frac{rL}{U}| \\ &\quad + Y'_{\beta\beta r} \beta^2 \frac{rL}{U} + Y'_{\beta rr} \beta |\beta| (\frac{rL}{U})^2) \\ N_H &= \frac{\rho}{2} L d U^2 (N'_\beta + N'_r \frac{rL}{U} + N'_{\beta\beta} \beta |\beta| + N'_{rr} \frac{rL}{U} |\frac{rL}{U}| \\ &\quad + N'_{\beta\beta r} \beta^2 \frac{rL}{U} + N'_{\beta rr} \beta |\beta| (\frac{rL}{U})^2)\end{aligned}\quad (2)$$

where ρ is the water density; L denotes the length over all of ship; d is the draught of ship; U represents the speed of ship. The hydrodynamic coefficients ($X'_{\beta r}, X'_{uu}, \dots, N'_{\beta rr}$) can be estimated with the method described in [26].

The propeller mainly produces longitudinal force, and its lateral force is negligible. Thus propeller hydrodynamic model can be written as:

$$\begin{aligned} X_P &= (1 - t_P)T \\ Y_P &= 0 \\ N_P &= 0 \end{aligned} \tag{3}$$

where t_P is a coefficient, and the propeller thrust force T is defined:

$$T = \rho n^2 D_p^4 k_T \tag{4}$$

132 where n is propeller speed (rpm); D_p is diameter of the propeller; k_T is the
133 thrust coefficient.

The hydrodynamic forces and moment generated by the rudder can be calculated by the following formula:

$$\begin{aligned} X_R &= - (1 - t_R)F_N \sin \delta \\ Y_R &= - (1 + a_H)F_N \cos \delta \\ N_R &= - (x_R + a_H x_H)F_N \cos \delta \end{aligned} \tag{5}$$

134 where t_R , a_H are coefficients; x_R and x_H are the distances from the rudder
135 and the propeller to the ship's center of gravity, respectively; F_N is the rudder
136 pressure; δ denotes the rudder angle.

137 3.3. Wind force model

The wind has a significant effect on the ship, which will affect heading and sway movement. Failure to compensate correctly for wind during docking is one of the main factor of docking accidents. Here, the wind forces and moments acting on the ship are estimated as [27]:

$$\begin{aligned} X_W &= \frac{1}{2} C_X \rho_a V_r^2 A_F \\ Y_W &= \frac{1}{2} C_Y \rho_a V_r^2 A_L \\ N_W &= \frac{1}{2} C_N \rho_a V_r^2 A_L L \end{aligned} \tag{6}$$

138 The physical meaning of each symbol in Eq.(6) is shown in Table 2.

Table 2: Parameters of wind force model

Symbol	Physical meaning
ρ_a	Air density
A_F	Frontal projected area of ship
A_L	Lateral projected area of ship
V_r	Relative wind speed
X_W	Fore-aft component of wind force
Y_W	Lateral component of wind force
N_W	Yawing moment
C_X, C_Y, C_N	Coefficients calculated using Isherwood72

139 4. Proposed approach

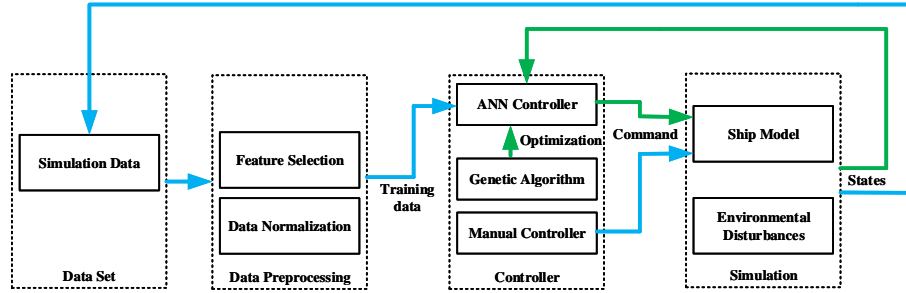


Figure 2: A neural-network based control strategy for automatic ship docking.

140 Fig. 2 schematically depicts the ANN-based ship docking control strategy
 141 for ship docking under environmental disturbances. First, the ship docking
 142 simulation module is constructed. It consists of a ship model and environmental
 143 disturbance models, which is fundamental to both manual control and ANN-
 144 based control. Based on that, training data set can be generated, as indicated
 145 by the blue arrow. The “data set” is the collection of ship manoeuvring

146 data from the simulation. The data is pre-processed through feature selection
 147 to find optimal input parameters for ANN construction, and further normalized
 148 before the training of the ANN. The green arrow illustrates the implementation
 149 of the ANN-based approach. The ANN is optimized by a genetic algorithm and
 150 trained using the data set. As a result, the trained ANN model can be applied
 151 to steer the ship to dock under external disturbances.

152 4.1. Data generation

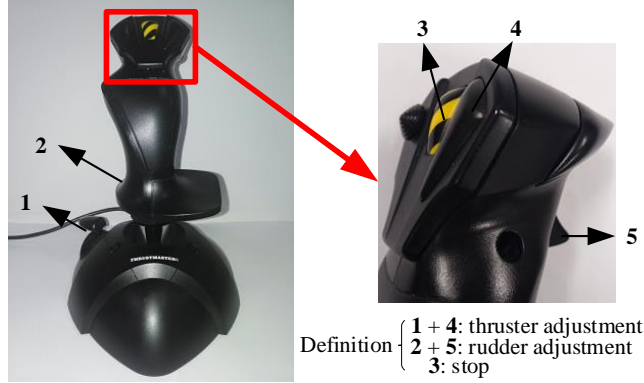


Figure 3: Definition of Joystick.

153 In this research, training data is created through “manual controller”, i.e.,
 154 by a skilled captain using a joystick to control ship’s rudder and thrust. The
 155 usage of the joystick is shown in Fig. 3. “Button 4” is used to enable the
 156 control of thruster speed. Only when it is pressed, can “Button 1” be used to
 157 adjust thruster speed within the range of $[-130, 130]RPM$. Similarly, “Button
 158 5” enables the use of rudder control, and “Handle 2” can adjust rudder angle
 159 between -45° and 45° only if “Button 5” is pressed. “Button 3” is the stop key.
 160 When the ship arrives at the dock safely, the captain can press the button to
 161 stop the maneuver.

162 4.2. Data pre-processing

The data pre-processing mainly contains two parts: feature selection and data normalization. The purpose of feature selection is to choose an optimal subset from the training data for ship control. In this paper, a step-wise feature selection method is developed. First, those constant variables would be deleted. In addition, to remove the redundant information between input parameters, Pearson correlation analysis [28] is applied. Then ANN-based variance-based sensitivity analysis is used for identifying the importance of each feature [29]. Assume any two input parameters x and y , the Pearson correlation of these two parameters can be defined as follows:

$$\rho_{xy} = \frac{\sigma_{xy}^2}{\sqrt{\sigma_x^2 \sigma_y^2}} \quad (7)$$

where σ_x is the standard deviation of x ; σ_x^2 is the variance of x ; σ_y is the standard deviation of y ; σ_y^2 is the variance of y ; σ_{xy}^2 is the co-variance of the variables x and y . The Pearson coefficient can be used to detect the dependency of two input parameters. In this paper, one of the two parameters would be removed, if the Pearson coefficient of the two parameters is large. If the model form is $f(\mathbf{X}) = f(x_1, \dots, x_M)$, where $\mathbf{X} = (x_1, \dots, x_M)$ represents the model input which contains M independent parameters. Based on the theory of Sobol [30], the variance-based sensitivity index can be described as the ratio of partial variance and total variance. The influence of the i -th variable x_i to the output can be defined by

$$S_{Ti} = 1 - \frac{V_{\sim i}}{V} \quad (8)$$

163 where S_{Ti} is the influence of input parameter to output; V stands for the total
 164 variance; and $V_{\sim i}$ represents the influence excluding the i -th variable. If the S_{Ti}
 165 is close to zero, the parameter can be considered to be non-important.

In addition, it is necessary to normalize all parameters to speed up the training convergence and improve accuracy of the ANN model. All the parameters would be normalized:

$$\hat{\mathbf{x}} = \frac{\mathbf{x} - E(\mathbf{x})}{\sqrt{Var(\mathbf{x}) + \epsilon}} \quad (9)$$

166 where $E(\mathbf{x})$ represents the mean of \mathbf{x} ; $Var(\mathbf{x})$ stands for the variance of \mathbf{x} ; ϵ is
 167 a positive infinitesimal to make the calculation possible when \mathbf{x} is a constant; ϵ
 168 is set to 10^{-6} in this paper.

169 4.3. ANN-based controller

Since the automatic ship docking system is a multi-input and multi-output system, it is important to design a neural network that can learn the underlying nature relationship between inputs and outputs autonomously. An ANN-based controller with two independent parallel structure is designed. The inputs of the ANN are the parameters selected from data analysis, and the outputs are the ship's propeller speed and rudder angle. The construction of the two parallel multi-layer ANN is demonstrated in Fig. 4. The ANN is a multilayer feedforward network that can be trained by error backpropagation. The principle of the

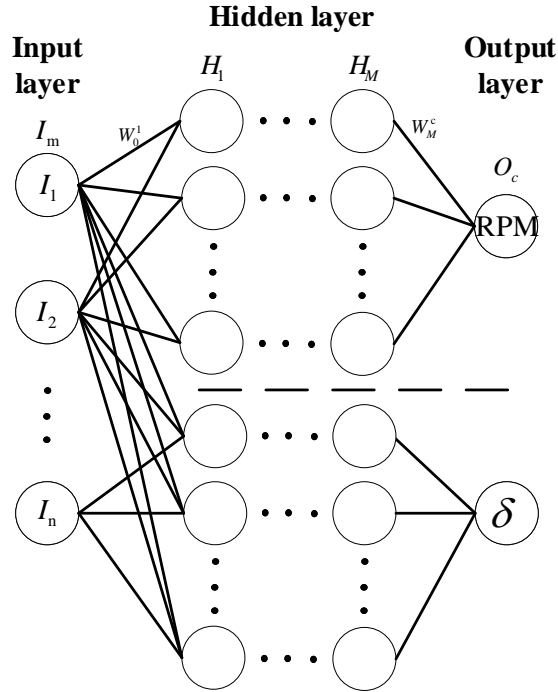


Figure 4: Multi-layer ANN with two parallel architecture.

training algorithm is the gradient descent method that is used to minimize the mean square error (MSE) between the actual output value of the network and the desired output value. Assume the neural network in Fig. 4 consists of an input layer, M hidden layers and an output layer. The output of each hidden layer can be written as:

$$H_i = f(W_{i-1}^i H_{i-1} + b_i), i = 1, 2, \dots, M \quad (10)$$

where $H_0 = I_m$, W_i^{i+1} is the weight between the hidden layers; b_i is the offset of the hidden layer; and f is activation functions. Here we choose the Tansig function as the activation function, and its mathematical expression is expressed as:

$$f(x) = \frac{2}{1 - \exp(-2x)} - 1 \quad (11)$$

Similarly, the output layer of ANN uses linear function, and its formula is expressed as following form:

$$O_c = \text{purelin}(W_n^c H_n + b_c) \quad (12)$$

where W_n^c is the weight between the last hidden layer and output layer; b_c is the offset; and H_n is the input of the output layer. The performance of the trained network is determined by calculating the value of the MSE. Suppose there are k samples in the training data, $(x_1, y_1), (x_2, y_2), \dots, (x_k, y_k)$, where (x_k, y_k) represent the inputs and outputs of the samples. The objective function of the network training is written as:

$$MSE = \frac{1}{k} \sum_{i=1}^k (y(i) - O_c)^2 \quad (13)$$

where $y(i)$ can be either rudder angle or propeller speed. The Levenberg-Marquardt algorithm is used to minimize the MSE. The weights of the ANN are updated as follows:

$$\begin{aligned} W_{i-1}^i(t) = & W_{i-1}^i(t-1) - [J^T(W_{i-1}^i(t-1))J(W_{i-1}^i(t-1)) \\ & + \mu I]^{-1} J^T(W_{i-1}^i(t-1))MSE(W_{i-1}^i(t)) \end{aligned} \quad (14)$$

170 where J is Jacobian matrix; and I is identity matrix.

171 In this paper, GA is used to optimize the ANN based controller. The chro-
 172 mosome consists of integers, representing the number of hidden layers and the
 173 number of neurons in each hidden layer [31]. The fitness function is designed as
 174 the performance of ANN in Eq.(13). Through GA operation including crossover
 175 and mutation, individuals with high fitness values will be selected to form a new
 176 generation. The process is repeated until termination condition is satisfied. As
 177 a result, the ANN structure is optimized to fit the training data.

178 5. Experiments

Table 3: Initial and Termination Ship States

Ship States	Initial	Termination
position x (m)	122	0
position y (m)	600	0
heading ψ ($^\circ$)	[0,360]	270
surge velocity u (m/s)	0	0
sway velocity v (m/s)	0	0
yaw velocity r (rad/s)	0	0

Table 4: PARAMETERS OF MODEL SHIP

Type	Length	Beam	Draught	Deadweight	A_F	A_L
Value	93(m)	23(m)	8(m)	4925($tonnes$)	470(m^2)	965(m^2)

179 This section is devoted to the validation of the proposed ANN-based ap-
 180 proach. First, a docking scenario is built up, as listed in Table 3. Then, for
 181 training the ANN, the data with three different environmental conditions, in-
 182 cluding no wind, constant wind and dynamic wind, is collected from a simulated

vessel, whose parameters are shown in Table 4. All experiments are conducted in a computer equipped with 2.60 GHz i7-6700K CPU and 16 GB RAM.

5.1. Feature selection

To obtain the optimal input parameters for the ANN shown in Fig. 4, the proposed feature selection method is performed. There are 16 parameters are logged in the simulated scenarios, mainly including two categories: state of vessel and environmental information. The vessel's state includes its position



Figure 5: Correlation analysis of 12 input parameters.

and heading, the speed of vessel in each DOF, the force of vessel in each DOF, and the state of thrusters; environmental information includes the force of wind in each DOF, the wind speed and the wind direction. Since wind speed and wind direction are constant values, they are removed for analysis. Thus, the correlation of 12 parameters excluding two output variables, i.e., rudder and thruster speed, are used for correlation analysis, as shown in Fig. 5. We further use a threshold $\rho_{xy} = 0.84$ to eliminate redundant information among parameters, which results in the removal of parameters “yaw speed”, “surge

force”, “sway force”, “yaw force”, “wind force of surge”, “wind force of sway”, and
“wind force of yaw”. An ANN used for sensitivity analysis is built on the basis
of the rest 5 parameters. A variance-based Sobol method with a distribution
sampled from the original data is performed on the ANN [29]. Fig. 6 shows the
sensitivity index of the 5 parameters.

From the sensitivity analysis, 3 input parameters, i.e., x, y, and heading
angle are selected as the inputs of the ANN with parallel structure for rudder
control, and 2 input parameters including x and y for the control of thruster
speed.

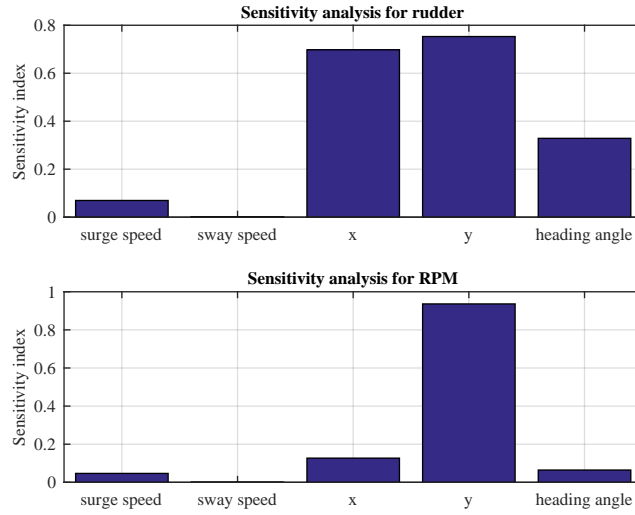


Figure 6: Sensitivity analysis for rudder and RPM.

5.2. Configuration of ANN

It is necessary to determine the structure of ANN, as there are no existing
rules that can be used to accurately select the number of layers of the hidden
layer and the number of neurons. In this study, the structure was determined
by trial and observation of the minimum MSE employing GA. The search for
the number of hidden layers is set as $M \in [2, 3, 4, 5, 6]$, and the search for
the number of neurons in each hidden layer is set as $N \in [0, 3, 6, 9, 12]$. The

Table 5: parameters for hidden layers after GA optimization

M	δ			Rpm		
	M_o	N	MSE	M_o	N	MSE
2	2	12, 12	1.100×10^{-3}	2	12, 12	3.800×10^{-3}
	2	12, 12	1.100×10^{-3}	2	12, 12	3.800×10^{-3}
3	3	12, 12, 12	8.388×10^{-4}	3	12, 12, 12	3.400×10^{-3}
	3	9, 9, 12	8.514×10^{-4}	3	12, 12, 12	3.400×10^{-3}
4	3	9, 12, 3	7.088×10^{-4}	4	12, 6, 12, 12	3.100×10^{-3}
	4	9, 9, 12, 6	7.547×10^{-4}	4	12, 6, 12, 12	3.100×10^{-3}
5	4	12, 12, 12, 12	5.976×10^{-4}	4	12, 6, 12, 6	3.100×10^{-3}
	5	12, 9, 12, 12, 12	5.673×10^{-4}	4	12, 6, 12, 12	3.100×10^{-3}
6	4	12, 12, 6, 12	6.430×10^{-4}	4	12, 12, 12, 12	3.200×10^{-3}
	4	12, 3, 12, 12	7.419×10^{-4}	5	12, 6, 3, 12, 12	3.200×10^{-3}

214 optimized hidden number M_o should meet the requirement $M_o \in M$. For GA,
 215 each chromosome contains the above two parameters, i.e. number of hidden
 216 layers and neurons. The crossover probability and mutation probability of GA
 217 are set to 0.3, and the stopping criterion is that the number of generations
 218 reaches 50. Table 5 lists the optimized hidden layers and the neuron number of
 219 each hidden layer. Considering both MSE and training time, four hidden layers
 220 with the corresponding neuron number shown in bold in Table 5 are used for
 221 the experiment.

222 5.3. Verification of ANN in no wind condition

223 Fig. 7 illustrates some successful maneuvers without wind perturbation in
 224 dotted lines using the ANN-based approach. Note the two paths one in red
 225 representing the trajectory using the same initial heading in training data; and
 226 the blue one representing a completely new initial heading different from the
 227 training data. The rudder angle and thruster speed generated completely by
 228 the ANN are expressed in Fig. 8. Fig. 9 illustrates the variation of the ship's
 229 surge velocity, sway velocity, yaw velocity and heading angle during the docking
 230 process. When the ship arrives at the dock, its velocities are very close to zero
 231 (less than 0.01 m/s), and the ship's heading angle is also approximately 270° .

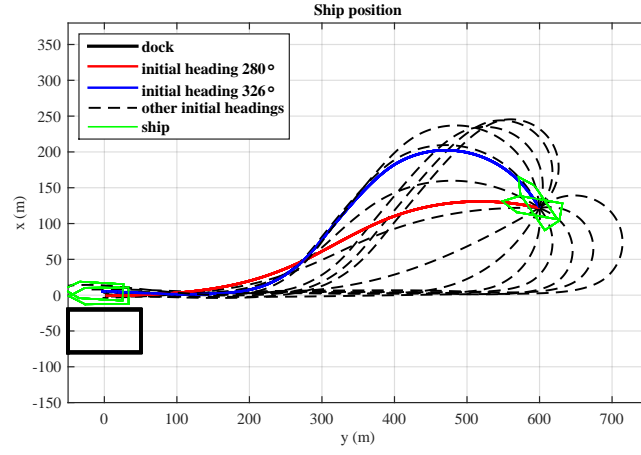


Figure 7: Docking results for different initial headings without wind.

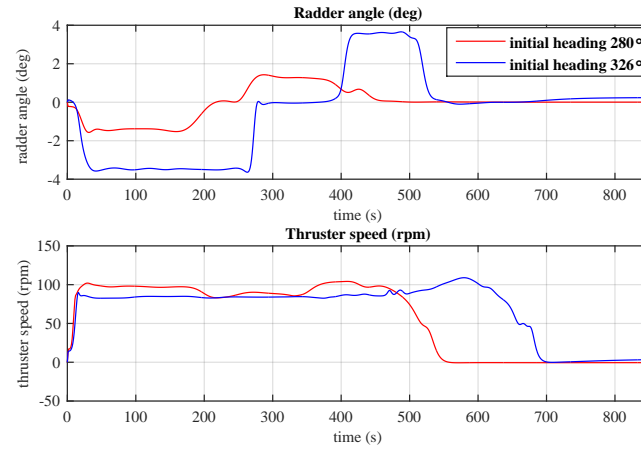


Figure 8: Rudder angle and thruster speed for maneuvers with initial heading of 280° and 326° under no wind.

232 In this case, the ship successfully stopped at the dock and terminal states also
 233 meet the requirements in Table 3.

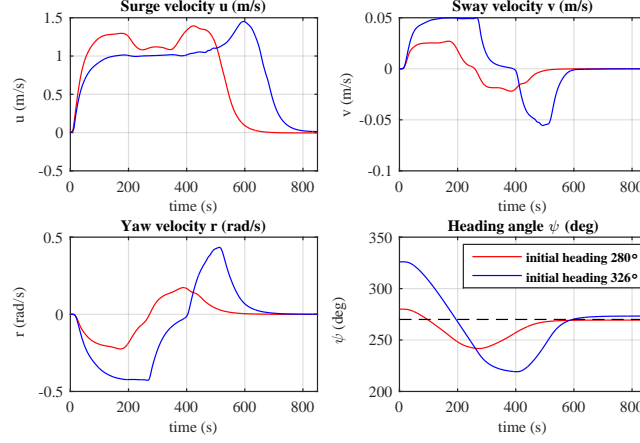


Figure 9: Ship velocities and heading angle for maneuvers with initial heading of 280° and 326° under no wind.

233

234 5.4. Verification of ANN in constant wind condition

235 Here we test the ANN-based controller in different initial states under con-
 236 stant wind condition of $V_w = 3m/s$ and $\beta_w = 0^\circ$.

237 Fig. 10 illustrates the automatic docking trajectory starting from different
 238 initial headings. The red curve and the blue curve are two successful maneuvers,
 239 with the same initial states and different initial states from the training set,
 240 respectively. The thruster speed dramatically fluctuates between 300 and 400
 241 seconds, which may be caused by speed adjustment. It can be seen from Fig. 12
 242 that when ships arrive at the dock, the surge velocity and yaw velocity are close
 243 to zero, and the heading angle is also close to 270° . Due to the disturbance of
 244 wind, the ship's sway velocity is not zero.

245 5.5. Verification of ANN in dynamic wind condition

246 The ANN-based controller is tested under different wind speeds. Fig. 13
 247 shows the results of different ship initial states. The red curve represents a ship

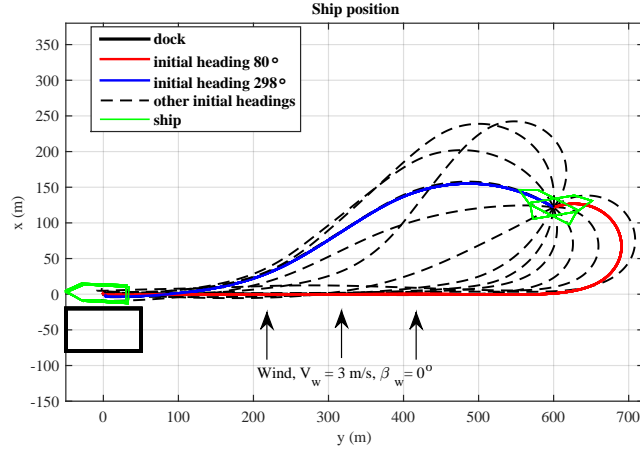


Figure 10: Docking results with different initial headings under constant wind.

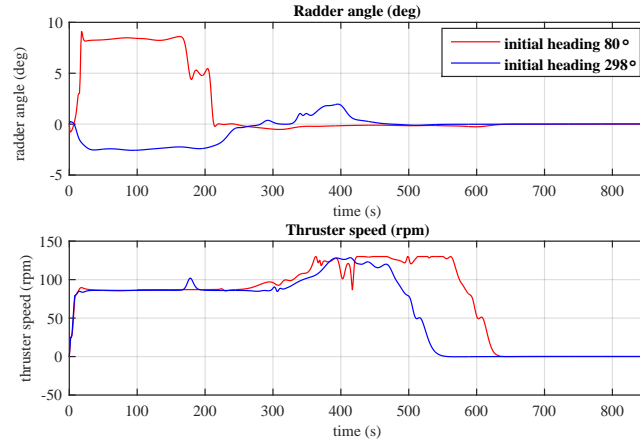


Figure 11: Rudder angle and thruster speed for maneuvers with initial heading of 80° and 298° under constant wind.

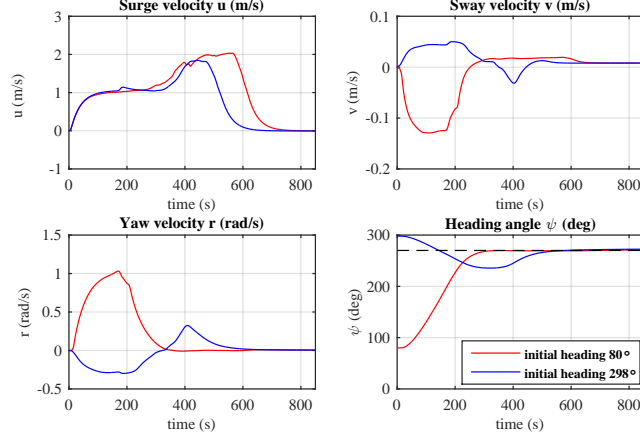


Figure 12: Ship velocities and heading angle for maneuvers with initial heading of 80° and 298° under constant wind.

248 docking path starting from heading 300° which is included in training data.
 249 The blue curve is a maneuver that the ship starts from a random heading. It
 250 shows that the ANN cannot navigate the ship to move straight when arriving
 251 at position $(0, 500)$, even though the ship is heading towards the dock. The
 252 reason is that the wind is becoming stronger at the moment. In the simulation,
 253 wind direction is constant ($\beta_w = 0^\circ$), and speed changes randomly from $1.5m/s$
 254 to $4.5m/s$ per minute, as demonstrated in the bottom panel of Fig. 14. The
 255 change of surge velocity, yaw velocity, and heading angle can converge to zero
 256 at last, but the sway velocity fluctuates periodically with the wind disturbance,
 257 as shown in Fig. 15.

258 5.6. Discussion

259 The simulation results show that in no wind condition, the ANN controller
 260 works very well, with only small fluctuations in command of rudder angle and
 261 thruster speed. Moreover, the ship states are in full compliance with the re-
 262 quirements in Table 3 when the ship arrives at its destination. Ships can also
 263 dock safely in the constant wind environment, but there is a slight error in the
 264 final heading angle (less than 2°) and the yaw speed is not fully zero. The main

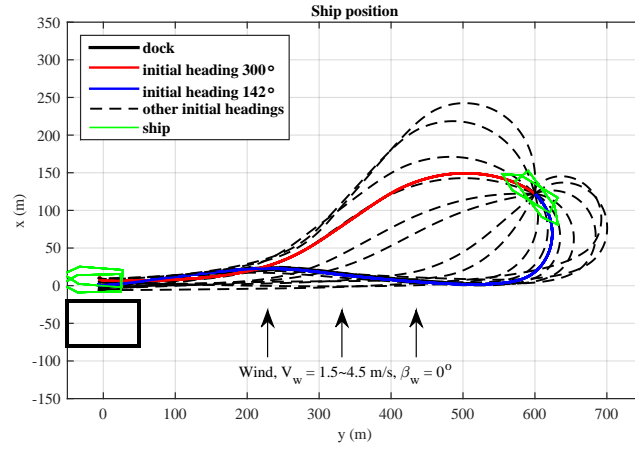


Figure 13: Docking results with different initial headings under dynamic wind.

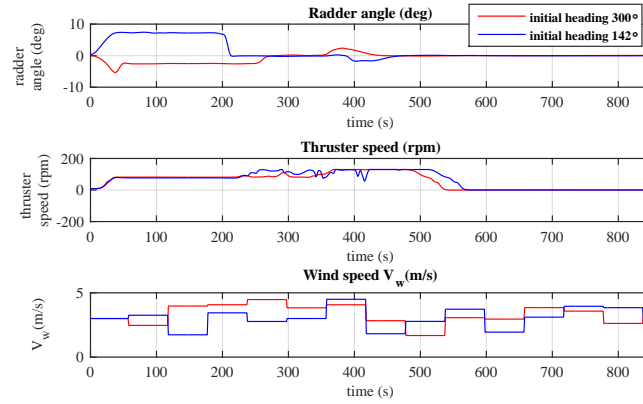


Figure 14: Rudder angle and thruster speed for maneuvers with initial heading of 300° and 142° under dynamic wind.

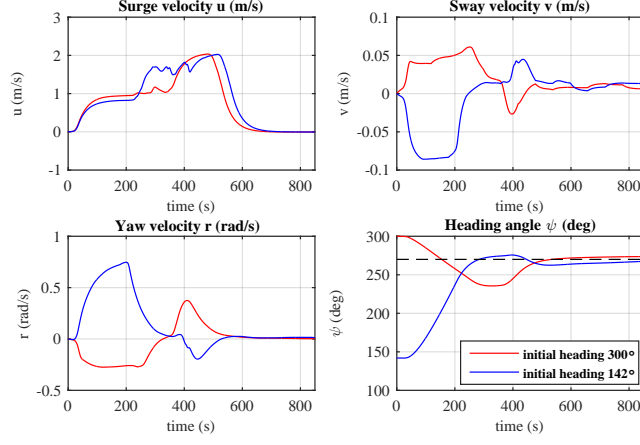


Figure 15: Ship velocities and heading angle for maneuvers with initial heading of 300° and 142° under dynamic wind.

reason for this problem is that the ship is required to sail at low speed when it approaches the berth, which greatly reduces the ship's maneuverability. In the dynamic wind condition, the control results of the ANN are not as good as these in the previous conditions due to the randomness of the wind. The rudder angle and propeller speed fluctuate drastically and the path is not smooth enough. In addition, the ship cannot successfully arrive the dock when it departs from initial heading angles between 5° and 23° . Because at these initial heading angles, the ANN is very sensitive to the disturbance of dynamic wind.

6. Conclusion

This research proposes a novel way to generate reliable ship docking data and finds the optimal variables for training a new neural network by employing feature selection technique and genetic algorithm which were not considered in previous studies. The conclusions of this work are summarized as follows:

- 1) A ship docking simulation module is established, which provides both manual and algorithm-based interface for ship docking operation.

- 280 2) Feature selection is applied to eliminate redundant information between
281 input parameters and identify their importance to ship's control param-
282 eters.
- 283 3) To ensure the stability of the ANN-based approach, the neural network
284 structure is optimized by using GA. Two parallel forward neural networks
285 with four hidden layers are established to control ship's rudder angle and
286 the propeller speed, respectively.
- 287 4) Numerical results show that under no wind and constant wind conditions,
288 the feasibility of the ANN-based approach is fully reflected; while under
289 the dynamic wind environment, the performance is inferior but can still
290 steer the ship into dock.

291 For future study, it is critical to improve the proposed approach to effec-
292 tively compensate for dynamic wind disturbances. In addition, advanced mech-
293 anisms will be set up to create versatile control strategies that meet different
294 requirements, such as minimum time maneuver, lowest energy consumption,
295 and collision avoidance with dynamic obstacles.

296 Acknowledgment

297 This work was partially supported by the project "Digital Twins for Vessel
298 Life Cycle Service" (Project no.: 280703), and partially by the project "Dynamic
299 Motion Planning Based on Trajectory Prediction in Close-range Manoeuvring"
300 (Project no.: 298399) in Norway.

301 References

- 302 [1] H. Katayama, H. Aoki, Straight-line trajectory tracking control for
303 sampled-data underactuated ships, IEEE Transactions on Control Systems
304 Technology 22 (4) (2014) 1638–1645.

- 305 [2] G. Li, W. Li, H. P. Hildre, H. Zhang, Online learning control of surface ves-
306 sels for fine trajectory tracking, *Journal of Marine Science and Technology*
307 21 (2) (2016) 251–260.
- 308 [3] N. Mizuno, N. Saka, T. Katayama, A ship’s automatic maneuvering sys-
309 tem using optimal preview sliding mode controller with adaptation mech-
310 anism, *IFAC-PapersOnLine* 49 (23) (2016) 576–581.
- 311 [4] D. Yingjie, Z. Xianku, Z. Guoqing, Fuzzy logic based speed optimization
312 and path following control for sail-assisted ships, *Ocean Engineering* 171
313 (2019) 300–310.
- 314 [5] T. A. Tran, X. Yan, Y. Yuan, Marine engine rotational speed control auto-
315 matic system based on fuzzy pid logic controller, in: 2017 4th International
316 Conference on Transportation Information and Safety (ICTIS), 2017, pp.
317 1099–1104.
- 318 [6] H. Yamato, Automatic berthing by the neural controller, *Proc. of Ninth*
319 *Ship Control Systems Symposium* 3 (1990) 3183–3201.
- 320 [7] Y. Zhang, G. E. Hearn, P. Sen, A multivariable neural controller for auto-
321 matic ship berthing, *IEEE Control Systems Magazine* 17 (4) (1997) 31–45.
- 322 [8] N. Im, K. Hasegawa, A study on automatic ship berthing using parallel
323 neural controller, *Journal of the Kansai Society of Naval Architects, Japan*
324 2001 (236) (2001) 65–70.
- 325 [9] N. Im, et al., A study on automatic ship berthing using parallel neural
326 controller (2nd report), *Journal of the Kansai Society of Naval Architects,*
327 *Japan* 2002 (237) (2002) 237_127–237_132.
- 328 [10] P.-H. Nguyen, Y.-C. Jung, Automatic berthing control of ship using adap-
329 tive neural networks, *Journal of Navigation and Port Research* 31 (7) (2007)
330 563–568.

- 331 [11] Q. Zhang, G. Zhu, X. Hu, R. Yang, Adaptive neural network auto-berthing
332 control of marine ships, *Ocean Engineering* 177 (2019) 40–48.
- 333 [12] N. Mizuno, M. Kuroda, T. Okazaki, K. Ohtsu, Minimum time ship ma-
334 neuvering method using neural network and nonlinear model predictive
335 compensator, *Control Engineering Practice* 15 (6) (2007) 757–765.
- 336 [13] G. Xu, K. Hasegawa, Automatic berthing system using artificial neural
337 network based on teaching data generated by optimal steering, in: *The*
338 *Japan Society of Naval Architects and Ocean Engineers*, 2012, pp. 295–
339 298.
- 340 [14] Y. A. Ahmed, K. Hasegawa, Automatic ship berthing using artificial neural
341 network based on virtual window concept in wind condition, *IFAC Proceed-*
342 *ings Volumes* 45 (24) (2012) 286–291.
- 343 [15] Y. A. Ahmed, et al., Automatic ship berthing using artificial neural network
344 trained by consistent teaching data using nonlinear programming method,
345 *Engineering applications of artificial intelligence* 26 (10) (2013) 2287–2304.
- 346 [16] Y. A. Ahmed, K. Hasegawa, Experiment results for automatic ship berthing
347 using artificial neural network based controller, *Ifac Proceedings Volumes*
348 47 (3) (2014) 2658–2663.
- 349 [17] Y. A. Ahmed, K. Hasegawa, Artificial neural network based automatic ship
350 berthing combining pd controlled side thrusters âĀĤ a combined controller
351 for final approaching to berth, in: *International Conference on Control*
352 *Automation Robotics and Vision*, 2015.
- 353 [18] N. Mizuno, et al., A shipâĀĤs minimum time maneuvering system using
354 neural network and non-linear model based super real-time simulator, *Pro-*
355 *ceedings of ECCâĀĤ03*.
- 356 [19] N. Mizuno, H. Kakami, T. Okazaki, Parallel simulation based predic-
357 tive control scheme with application to approaching control for automatic
358 berthing, *IFAC Proceedings Volumes* 45 (27) (2012) 19–24.

- 359 [20] N. Mizuno, Y. Uchida, T. Okazaki, Quasi real-time optimal control scheme
360 for automatic berthing, IFAC-PapersOnLine 48 (16) (2015) 305–312.
- 361 [21] N.-K. Im, V.-S. Nguyen, Artificial neural network controller for automatic
362 ship berthing using head-up coordinate system, International Journal of
363 Naval Architecture and Ocean Engineering 10 (3) (2018) 235–249.
- 364 [22] V.-S. Nguyen, V.-C. Do, N.-K. Im, Development of automatic ship berthing
365 system using artificial neural network and distance measurement system,
366 International Journal of Fuzzy Logic and Intelligent Systems 18 (1) (2018)
367 41–49.
- 368 [23] K. Kose, J. Fukudo, K. Sugano, S. Akagi, M. Harada, On a computer aided
369 maneuvering system in harbours, Journal of the Society of Naval Architects
370 of Japan 1986 (160) (1986) 103–110.
- 371 [24] T. I. Fossen, Handbook of marine craft hydrodynamics and motion control,
372 John Wiley & Sons, 2011.
- 373 [25] P. Committee, et al., Final report and recommendations to the 23rd ittc,
374 Proceeding of 23rd ITTC.
- 375 [26] K. Katsuro, et al., On the maneuvering performance of a ship with the
376 parameter of loading condition, Journal of the Society of Naval Architects
377 of Japan. The Japan Society of Naval Architects and Ocean Engineers (168)
378 (1990) 141–148.
- 379 [27] T. Fujiwara, M. Ueno, T. Nimura, Estimation of wind forces and mo-
380 ments acting on ships, Journal of the Society of Naval Architects of Japan
381 1998 (183) (1998) 77–90.
- 382 [28] S.-D. Bolboaca, L. Jäntschi, Pearson versus spearman, kendall’s tau cor-
383 relation analysis on structure-activity relationships of biologic active com-
384 pounds, Leonardo Journal of Sciences 5 (9) (2006) 179–200.

- 385 [29] X. Cheng, G. Li, R. Skulstad, P. Major, S. Chen, H. P. Hildre, H. Zhang,
386 Data-driven uncertainty and sensitivity analysis for ship motion modeling
387 in offshore operations, *Ocean Engineering* 179 (2019) 261–272.
- 388 [30] A. Saltelli, I. M. Sobol', Sensitivity analysis for nonlinear mathemati-
389 cal models: numerical experience, *Matematicheskoe Modelirovanie* 7 (11)
390 (1995) 16–28.
- 391 [31] A. V. Phan, M. Le Nguyen, L. T. Bui, Feature weighting and svm param-
392 eters optimization based on genetic algorithms for classification problems,
393 *Applied intelligence* 46 (2) (2017) 455–469.